NIH Public Access
Author Manuscript
Exp Eye Res. Author manuscript; available in PMC 2013 August 28.

Published in final edited form as:
Exp Eye Res. 2009 March ; 88(3): 367–377. doi:10.1016/j.exer.2008.07.012.

Anti-sphingosine-1-phosphate monoclonal antibodies inhibit angiogenesis and sub-retinal fibrosis in a murine model of laser-induced choroidal neovascularization

Sergio Caballero[a], **James Swaney**[b], **Kelli Moreno**[b], **Aqeela Afzal**[a], **Jennifer Kielczewski**[a], **Glenn Stoller**[b,c], **Amy Cavalli**[b], **William Garland**[b], **Geneviève Hansen**[b], **Roger Sabbadini**[b,d], and **Maria B. Grant**[a,*]

[a]Department of Pharmacology & Therapeutics, University of Florida, Gainesville, FL, USA

[b]Lpath Inc., San Diego, CA 92121, USA

[c]Ophthalmic Consultants of Long Island, Lynbrook, NY 11563, USA

[d]Department of Biology, San Diego State University, San Diego, CA 92182, USA

Abstract

The efficacy of novel monoclonal antibodies that neutralize the pro-angiogenic mediator, sphingosine-1-phosphate (S1P), were tested using in vitro and in vivo angiogenesis models, including choroidal neovascularization (CNV) induced by laser disruption of Bruch's membrane. S1P receptor levels in human brain choroid plexus endothelial cells (CPEC), human lung microvascular endothelial cells, human retinal vascular endothelial cells, and circulating endothelial progenitor cells were examined by semi-quantitative PCR. The ability of murine or humanized anti-S1P monoclonal antibodies (mAbs) to inhibit S1P-mediated microvessel tube formation by CPEC on Matrigel was evaluated and capillary density in subcutaneous growth factor-loaded Matrigel plugs was determined following anti-S1P treatment. S1P promoted in vitro capillary tube formation in CPEC consistent with the presence of cognate $S1P_{1–5}$ receptor expression by these cells and the S1P antibody induced a dose-dependent reduction in microvessel tube formation. In a murine model of laser-induced rupture of Bruch's membrane, S1P was detected in posterior cups of mice receiving laser injury, but not in uninjured controls. Intravitreous injection of anti-S1P mAbs dramatically inhibited CNV formation and sub-retinal collagen deposition in all treatment groups ($p < 0.05$ compared to controls), thereby identifying S1P as a previously unrecognized mediator of angiogenesis and subretinal fibrosis in this model. These findings suggest that neutralizing S1P with anti-S1P mAbs may be a novel method of treating patients with exudative age-related macular degeneration by reducing angiogenesis and sub-retinal fibrosis, which are responsible for visual acuity loss in this disease.

Keywords

sphingosine; anti-angiogenesis; age-related macular degeneration; choroidal neovascularization; fibrosis; animal model

*Corresponding author. Department of Pharmacology & Therapeutics, P.O. Box 100267, Gainesville, FL 32610-100267, USA. grantma@ufl.edu (M.B. Grant).

NIH-PA Author Manuscript
NIH-PA Author Manuscript
NIH-PA Author Manuscript

NIH-PA Author Manuscript

NIH-PA Author Manuscript

NIH-PA Author Manuscript

1. Introduction

Age-related macular degeneration (AMD), the most common cause of adult blindness in developed countries, is complicated by choroidal neovascularization (CNV) and subsequent bleeding and exudation beneath the macula, which lead to severe vision loss and, ultimately, blindness. Both genetic and environmental factors influence the development of CNV. Although the exact pathogenesis of CNV is not known, chronic inflammation adjacent to the retinal pigmented epithelium (RPE), Bruch's membrane, and choriocapillaris appears to play a crucial role in CNV (Augustin and Offermann, 2006; Zarbin, 2007). Current clinical strategies for treating CNV are primarily aimed at reducing VEGF levels in the eye. However, other angiogenic and inflammatory mediators contribute to CNV either directly via activation of their cognate receptors, or indirectly via crosstalk with vascular endothelial growth factor (VEGF) and other signaling pathways. Thus, new therapies that interfere with VEGF, as well as other signaling pathways that promote angiogenesis, vascular leakage and inflammation would represent a significant advance in disease treatment.

Current therapies focus exclusively on inhibition of VEGF with two recently marketed anti-VEGF agents, pegaptanib (Macugen, OSI/Pfizer) (Ferrara et al., 2006) and ranibizumab (Lucentis, Genentech) (Ferrara et al., 2006; Rosenfeld et al., 2006), demonstrating efficacy as treatments for AMD. Despite the real advance that Lucentis represents, mean visual acuity improved only seven letters in the MARINA and 11 letters in the ANCHOR trials. Baseline acuity for MARINA was 20/80 and for ANCHOR 20/125; this translates to about a 20/70+ acuity at 24 months in MARINA and 20/80+ in ANCHOR. Therefore, the average patient who had a successful anti-angiogenic response to treatment did not regain driving vision or the ability to read without low-vision aids in the treated eye. In addition, although about 40% of all patients were 20/40 at the conclusion of the study, 60% of these patients did not have normal driving or normal reading vision (Ferrara et al., 2006). Thus, an unmet medical need for the development of novel therapeutic modalities for the treatment of exudative AMD remains and development of agents targeting signaling pathways distinct from VEGF or acting synergistically with anti-VEGF-based therapies could represent a more effective treatment strategy.

The bioactive lipid signaling mediator, sphingosine-1-phosphate (S1P) may represent just such a novel therapeutic target (Gardell et al., 2006). S1P is a small (<400 Da) extracellular, sphingolipid, signaling growth factor with pleiotropic actions mediated by a complement of five high-affinity G protein-coupled receptors ($S1P_{1–5}$, also known as EDG1–5) specific for the ligand (Anliker and Chun, 2004; Gardell et al., 2006).

S1P is involved in the regulation of a variety of cellular processes, including proliferation, migration, survival, cytoskeletal organization, adherens junction assembly, and morphogenesis in multiple cell lineages, including endothelial cells (Ozaki et al., 2003), fibroblasts (Watterson et al., 2007), and immune cells (Cyster, 2005; Olivera and Rivera, 2005). As a consequence, S1P is pro-angiogenic, pro-inflammatory and pro-fibrotic.

A critical component of S1P's biosynthetic pathway is sphingosine kinase type 1 (SphK1) which phosphorylates sphingosine to produce S1P. This isoform of the kinase is thought to be responsible for the release of S1P into the extracellular compartment. Recent evidence demonstrates that SPHK is expressed in retinal endothelial cells (Maines et al., 2006). Furthermore, S1P receptors are expressed by vascular endothelial cells (Chae et al., 2004; Maines et al., 2006; Sanchez and Hla, 2004; Sanchez et al., 2007) and, in particular, murine choroidal vasculature.(Sanchez et al., 2007). A knock out of $S1P_2$ receptors has been shown to mitigate vascular growth and permeability in the murine model of oxygen-induced retinopathy (Skoura et al., 2007). These data suggest that S1P may not only promote CNV

NIH-PA Author Manuscript

NIH-PA Author Manuscript

NIH-PA Author Manuscript

lesion growth but also permeability. Following the finding that SphK1 is expressed in retinal endothelial cells, Maines et al. (2006) established that intraperitoneal administration of SphK1 inhibitors could decrease vascular leakage in a rat model of streptozotocin-induced diabetic retinopathy. This is not surprising since a role for S1P has been well-established in non-retinal endothelial cell systems. For example, S1P promotes vascular leakage (Sanchez et al., 2007), proteolytic degradation of the extracellular matrix (Bayless and Davis, 2003; Bernatchez et al., 2003; Langlois et al., 2004; Lee et al., 2000), endothelial cell differentiation (Augustin and Offermann, 2006) and proliferation (Ferrara et al., 2006; Kee et al., 2005; Lee et al., 2000; Radeff-Huang et al., 2004), cell survival from migration-induced stress (Ferrara et al., 2006; Kee et al., 2005; Langlois et al., 2004; Limaye et al., 2005), and finally, assembly, alignment and adhesion to form the tubular structures of new vessels (Garcia et al., 2001; Li et al., 2004). As an angiogenic mediator, S1P is comparable to basic fibroblast growth factor (FGF-2) and VEGF in promoting vessel growth, and synergizes with these factors to promote development of vascular network in vivo (Ferrara et al., 2006; Igarashi et al., 2003; Spiegel and Milstien, 2003).

Thus, the S1P signaling system represents an attractive target for therapeutic intervention in ocular disease models where inappropriate angiogenesis and/or vascular leakage are involved. Inactivation of S1P signaling might provide additional therapeutic benefit by addressing the inflammatory and fibrotic component of this disease process. An anti-S1P murine mAb, designated LT1002, was recently developed with high binding affinity and specificity to S1P (Visentin et al., 2006). This anti-S1P mAb demonstrated significant anti-neovascularization effects using in vitro and in vivo assays.(Sabbadini, 2006; Visentin et al., 2006) Furthermore, LT1002 slowed tumor progression and reduced tumor vascularization in several murine models of human cancer. The murine mAb has recently been humanized (designated LT1009) and is currently in Phase 1 clinical trials for cancer as an anti-angiogenic agent.

In this report we show, for the first time, that laser rupture of Bruch's membrane increases local expression of S1P in the sub-retinal space. Intravitreous administration of either murine or humanized anti-S1P monoclonal antibodies (mAbs) potently attenuated CNV lesion volumes. Human endothelial cell from various vascular beds, including brain choroidal plexus (CPEC), lung microvascular (LMEC), retinal vascular (HREC) endothelial cells, and circulating endothelial precursor cells express $S1P_{1–5}$ receptors, and CPEC respond to anti-S1P mAbs with reduced angiogenesis in the matrigel tube formation assay. Thus, neutralization of S1P with anti-S1P mAbs may provide an effective, novel treatment of AMD and related ocular disorders where S1P is involved in disease progression.

2. Materials and methods

2.1. Anti-S1P antibodies

Murine and humanize IgGk1 mAb against S1P were obtained from Lpath, Inc. (San Diego, CA). These high affinity mAbs have been shown to be highly specific for S1P (Visentin et al., 2006); in the same study, the murine anti-S1P mAb (designated LT1002) showed efficacy as an anti-angiogenic agent in multiple in vivo models (Visentin et al., 2006). The humanized mAb (LT1009) showed similar specificity and affinity for S1P as the target when compared to the murine mAb (data not shown). For control experiments, a non-specific, isotype-matched murine mAb or isotype matched human IgGk1 was used (Strategic BioSolutions, Newark, DE).

2.2. Real time relative RT-PCR of S1P receptor expression in endothelial cells

S1P receptor gene expression was examined in human endothelial cells from three diverse vascular beds, as well as in circulating endothelial precursor cells. HREC were isolated from

NIH-PA Author Manuscript

NIH-PA Author Manuscript

NIH-PA Author Manuscript

donor eye tissue and grown as previously described (Grant and Guay, 1991). Primary human CPEC were obtained from ScienceCell Research Laboratories (San Diego, CA) and maintained as recommended. LMEC were purchased from Lonza, Inc. (Allendale, NJ) and maintained according to manufacturer's recommendations. Circulating endothelial progenitor cells (EPC) identified by CD34 expression were isolated and maintained as previously described (Caballero et al., 2007; Chang et al., 2007).

Total mRNA from each of these cell types was isolated using the total RNA Mini Kit (Bio-Rad, Hercules, CA). The mRNA was transcribed using an iScript cDNA Synthesis Kit (BioRad), and real-time PCR was performed using ABI Master Mix (ABI Biosystems, Foster City, CA). Pre-designed primers for S1P receptors ($S1P_{1–5}$) and α-actin were purchased from ABI Biosystems. All samples were normalized to α-actin. Real-time PCR was performed on an ABI Fast PCR machine for 60 cycles (ABI Biosystems). All reactions were performed in triplicate.

2.3. In vitro matrigel neovascularization assay

The ability of S1P to promote microvessel development in Matrigel was examined essentially as described previously (Visentin et al., 2006) with the following modifications: CPEC were starved overnight in DMEM 2% FBS and 1 mg/mL BSA. Matrigel (BD Biosciences Franklin Lakes, New Jersey) was diluted 1:2 with 2% FBS and 1 mg/mL BSA and 300 mL was placed in each well of a 24 well plate. A total of 5×10^4 cells/well were exposed for 30 min to either 10 nM S1P alone or with LT1002 or LT1009, and then plated onto the Matrigel-coated wells. The wells were examined every hour and photographed using a phase contrast scope.

2.4. In vivo Matrigel plug assay

Matrigel Matrix High Concentration was purchased from BD BioSciences (Franklin Lakes, NJ) and mixed with 50 ng/mL VEGF, 50 ng/mL FGF-2, and 3 ng/mL heparin as the angiogenic stimuli used for this study. Female C57BL/6 mice 6–8 weeks of age were divided into five treatment groups with five mice per group. All animal studies were performed under a protocol approved by the Institutional Animal Care and Use Committee at Southern Research Institute. On day 0, each animal was inoculated with 500 μL ice-cold Matrigel matrix plug to each left and right side of their flanks. One group served as a control receiving saline beginning one day prior to the implantation of the Matrigel plugs; the four other groups received drug treatment consisting in equal volumes of 0.33–81 mg/kg LT1009. All treatments were administered intraperitoneally every other day. Mice were euthanized at day 14 and plugs were collected from each group of mice by pulling back the mouse skin to expose the plug. Plugs were dissected out of the skin and fixed for histological analysis. Sections (5 μm) from paraffin-embedded plugs were stained with anti-CD-31 and blood vessel density was analyzed in a cross sectional area of each Matrigel plug. For each treatment group, a minimum of six Matrigel plugs were quantitatively analyzed to assess microvessel density.

2.5. Quantification of CNV in the laser injury murine model

Female C57Bl6/J mice of 10–12 weeks of age were purchased from Jackson Laboratories (Bar Harbor, ME). All animal studies were performed under a protocol approved by the Institutional Animal Care and Use Committee at the University of Florida, and in accordance with the ARVO Statement for the Use of Animals in Ophthalmic and Vision Research.

For the induction of CNV, animals were anesthetized with a mixture of ketamine (14 mg/kg) and xylazine (30 mg/kg) in sterile saline administered intraperitoneally at a dose of 100 mL

NIH-PA Author Manuscript

NIH-PA Author Manuscript

NIH-PA Author Manuscript

per 20 g of body weight. Their pupils were then dilated with one drop each of ophthalmic tropicamide (0.5%) and phenylephrine (2.5%). An argon green ophthalmic laser (Oculight GL 532 nm, Iridex Corporation, Mountain View, CA) coupled to a slit lamp set to deliver a 100 ms pulse at 200 mW with a 50 μm spot size was used to rupture Bruch's membrane in three quadrants of the right eye located approximately 50 μm from the optic disc at relative positions of 9, 12 and 3 o'clock. The left eye served as an uninjured control in all cases. The anti-S1P (LT1002, LT1009, or non-specific isotype control) was administered into the injured eye by intravitreous injection of 0.5 μg of antibody in 2 mL of vehicle (PBS) immediately following laser injury. Injections were repeated at weekly intervals for the duration of the studies. A model 1801RN 10 mL Hamilton syringe (Fisher Scientific, Orlando, FL) with a 32-gauge, 10 mm, point style 4 needle (custom made by the Hamilton Company, Reno, NV) was used to deliver the injection. A fresh, sterile syringe and needle combination was used for each separate agent to avoid cross contamination.

Choroidal neovascularization was evaluated as previously reported (Sengupta et al., 2003) Briefly, animals from each treatment cohort were euthanized by overdose of ketamine–xylazine mixture, and then underwent whole body perfusion via cardiac puncture with 6 ml 4% paraformaldehyde in PBS, pH 7.5. The eyes were enucleated, punctured with a 27 gauge needle 1 mm posterior to the limbus, and immersed in fixative for 1 h at room temperature, then washed two times by immersion in PBS buffer for 30 min. Eyes were then prepared for morphometry and volumetric measurement of CNV lesions as follows. The eyes were dissected to isolate the posterior segment consisting of the retinal pigment epithelium, the choriocapillaris and the sclera. This tissue was permeabilized and reacted with rhodamine-conjugated *Ricinus communis* agglutinin I (Vector Laboratories, Burlingame, CA) to detect the vessels within the CNV lesion. The posterior cups were cut with 4–7 radial slices, and mounted flat on microscope slides with a drop of Vectashield anti-fade medium (Vector Laboratories) for digital image capture by epifluorescence Zeiss Axioplan 2 with RGB Spot high-resolution digital camera and laser scanning confocal microscopy (BioRad MRC 1024, BioRad Corporation, Temecula, CA).

Captured digital images were evaluated morphometrically using ImageJ software (Research Services Branch, National Institutes of Health, Bethesda, MD). Each confocal z-series image capture of the red channel was analyzed as follows: (1) a calibration for the specific objective and microscope was applied to set the pixel-to-length ratio; (2) a threshold was applied using the Otsu algorithm; (3) images were made binary; (4) a region-of-interest (ROI) was outlined to include the entire lesion area; (5) a particle analysis was performed to quantify the pixel area above the threshold level within the ROI. The sum of lesion area throughout the *z*-series was then multiplied by the *z* thickness (typically 4 μm) to obtain the lesion volume. The three lesion volumes for each animal were then averaged and treated as an *n* of 1 for statistical analysis. Changes in lesion volume among treatment groups were determined by averaging the mean lesion volume for all animals in a treatment group, and reported as mean ± standard error from the mean. Comparisons are tested for statistical significance by Student's *t*-test or one-way analysis of variance (ANOVA). Differences in lesion volume with a *p* value less than or equal to 0.05 were considered significant.

In the first study, we evaluated LT1002 over a four-week time course of lesion development and regression with antibody treatment. For these studies, eyes were harvested for measurement of CNV lesion volume as described above and were also analyzed for collagen content as described below. In a second set of experiments, we compared the efficacy of LT1002 to the humanized anti-S1P mAb, LT1009, at 28 days after injury. For these latter studies, we confined our examination to the effects of these antibodies on CNV.

NIH-PA Author Manuscript

NIH-PA Author Manuscript

NIH-PA Author Manuscript

2.6. Collagen staining of CNV lesions

Selected mouse eyes from each treatment group (LT1002 treated or control antibody treated) and from each time point of 7, 14, and 28 days ($n = 3$ animals per treatment group for each time point) were fixed by immersion in Trump's fixative overnight, followed by three changes into PBS, after which they were embedded in paraffin and the blocks sectioned. The entire globes were cut at 8 μm per section, collecting every tenth section onto coated microscope slides (SuperfrostPlus, Fisher Scientific, Orlando, FL). The sections were then stained using Masson's Trichrome (Dako Corp., Carpenteria, CA) and digital images of each entire section were captured. The calibrated images were then examined by masked observers who selected the sections that showed the largest lesion diameter. To determine collagen deposition (scar formation) within the CNV lesion, the cross-sectional area (μm^2) of Trichrome staining within each sequential section was measured using ImageJ and the values from all sections were averaged to determine representative collagen deposition within the entire CNV lesion, and analyzed statistically as described above.

2.7. Immunohistochemical detection of S1P in CNV lesions

Immunohistochemical analysis of flat-mounts of posterior cups and ocular cross-sections was performed to assess S1P staining in control mouse retinas and retinas following laser-induced rupture of Bruch's membrane. For flat-mounts, tissue that had previously been stained with *R. communis* agglutinin I (Vector Laboratories) was subsequently incubated with LT1009 (40 μg/ml) diluted in PBS/ 1.0% BSA. Tissue was washed in PBS and then incubated with FITC-conjugated goat anti-human IgG (4 μg/ml) diluted in PBS. Tissue was washed and then mounted using Vectashield anti-fade medium. All antibody incubation and wash steps were conducted overnight at 4 °C.

2.8. Determination of S1P in vitreous fluid by S1P ELISA

S1P levels in rabbit vitreous were determined by competition ELISA. All rabbit studies were performed under a protocol approved by the Institutional Animal Care and Use Committee at IVD Services (Swanville, MN), and in accordance with the ARVO Statement for the Use of Animals in Ophthalmic and Vision Research. S1P coating material was diluted to 1.0 μg/mL as protein conjugate in carbonate buffer (100 mM $NaHCO_3$, 33.6 mM Na_2CO_3, pH 9.5). Plates were coated with 100 mL/well of coating solution and incubated at 37 °C for 1 h. The plates were then washed four times with PBS (100 mM Na_2HPO_4, 20 mM KH_2PO_4, 27 mM KCl, 1.37 mM NaCl, pH 7.4) and blocked with 150 μL/well PBS + 0.1% BSA and 0.01% Tween-20 for 1 h at room temperature. S1P standards were prepared by diluting 100 mM stock S1P into delipidized human serum (DHS) at the following concentrations: 2, 1, 0.5, 0.1, 0.01, and 0.0 μM. Samples were diluted appropriately so that the optical densities (OD) fell within the linear range of the standard curve (0.5–0.1 μM). Optimum dilutions for rabbit vitreous were found to be from 1:1 to 1:5 in DHS. The primary antibody (biotinylated anti-S1P mAb) was diluted to 0.8 μg/ml in PBS + 0.1% Tween-20 and combined with the samples or standards at a 1:3 ratio of antibody to sample on a non-binding plate (usually 100 μL Ab and 300 μL samples/ standards, enough to run in triplicate). The plates were then washed four times with PBS and then incubated for 1 h at room temperature with 100 μL/ well of the primary antibody combined with the samples/standards. Next the plates were washed 4× with PBS and then incubated for 1 h at room temperature with 100 μL/ well of HRP-conjugated streptavidin diluted 1:60,000 in PBS with 0.1% BSA and 0.01% Tween-20. The plates were washed again four times with PBS and developed using 100 μL/well TMB substrate at 4°C. After 8 min, the reaction was stopped with 1 M H_2SO_4, 100 μL/well. Optical densities were measured at 450 nm. Data were analyzed using Graphpad Prizm software. The standard ODs were graphed using a four parameter equation and used to calculate the S1P in the samples. Excel software was used to calculate the S1P concentration in each sample by correcting the values for the dilution factor.

NIH-PA Author Manuscript

NIH-PA Author Manuscript

NIH-PA Author Manuscript

2.9. Statistical analyses

In the time course study using the laser injury CNV model, the efficacy of LT1002 was tested in 36 animals. One-half of the mice were injected with non-specific antibody while the other half received LT1002 as described above. Six animals from each treatment group were euthanized at days 7, 14 and 28 following laser injury. The eyes ($n = 6$) from these animals were then further allocated evenly for assessment of either CNV lesion volume or collagen deposition as described above. Thus, each time/treatment value reported is derived from $n = 3$ animals for the time course study.

Additional studies comparing the effect of LT1002 vs. the humanized LT1009 on CNV lesion volume were conducted at day 28 post injury. Reported values were derived from $n = 15$ for non-specific antibody, $n = 16$ for LT1002, and $n = 14$ for LT1009.

All results are expressed as the mean ± SEM. The values were processed for statistical analyses by ANOVA followed by *t*-test assuming unequal variances using statistical analysis software (SPSS, Chicago, IL). Differences were considered statistically significant at $p < 0.05$.

3. Results

3.1. Ocular S1P levels

Table 1 shows that S1P can be detected within the vitreous fluid of healthy rabbits. As measured by a competitive ELISA assay, the concentration of S1P in the vitreous was substantial (120 nM) and exceeds the K_d for S1P receptors (~8–70 nM), but not as high as the levels found in rabbit plasma (~1000 nM). Rabbit vitreous was used because of the limited amount of vitreous fluid that can be obtained from mouse eyes, which would preclude making these measurements from mouse vitreous fluid.

3.2. S1P receptor gene expression

When measured by quantitative RT-PCR as shown in Fig. 1, the dominant isoforms of S1P receptors expressed by HREC and CPEC are $S1P_2$ and $S1P_3$. While $S1P_3$ is the predominant isoform expressed by CPEC, at levels more than 150-fold higher than $S1P_1$, HREC and CPEC are similar in that both $S1P_2$ and $S1P_3$ are expressed at significantly higher levels than $S1P_1$. $S1P_4$ and $S1P_5$ are not appreciably expressed by either HREC or CPEC.

The expression profile differs significantly for the other endothelial cell types examined. Human LMEC express primarily $S1P_1$, with very low expression of $S1P_{3–5}$. Circulating human EPC shows a pattern similar to the LMEC, with $S1P_1$ being the predominant receptor expressed, little or no expression of $S1P_3$ and $S1P_5$, and modest expression of $S1P_4$. These results show that human vascular endothelial cells and their precursors express mRNA for $S1P_{1–5}$ at markedly different levels depending on the vascular bed of origin.

3.3. In vitro and in vivo angiogenesis inhibition by LT1009

Consistent with the finding that CPECs express S1P receptors, Fig. 2 shows that S1P was capable of stimulating the microvessel formation by CPEC in the Matrigel tube formation assay. S1P stimulated tube formation at both the 1 and 10 nM concentration with greatest degree of tube formation occurring at 10 nM in this in vitro assay (Fig. 3A and B). Using this concentration, we observed robust tube formation within the first 8–12 h followed by slight regression of the tubes at 24 h. We next tested the effect of the humanized anti-S1P mAb, LT1009 (25 and 50 μg/mL) on S1P-mediated tube formation and found that CPEC exposed to LT1009 demonstrated a dose-dependent regression in microvessel tube

NIH-PA Author Manuscript

NIH-PA Author Manuscript

NIH-PA Author Manuscript

formation (Fig. 2C and D). Although cell viability was normal, no spontaneous tube formation was observed in the model with unstimulated CPEC (Fig. 2F).

These findings were recapitulated in the in vivo Matrigel plug assays (Fig. 3). Matrigel plugs containing optimum concentrations of VEGF (50 ng/mL) and FGF-2 (50 ng/mL) were implanted in female C57BL/6 mice. As can be seen in the Fig. 3B, these pro-angiogenic growth factors promoted substantial increases in microvessel density (MVD) as measured by CD-31 staining (see Section 2). Systemic administration of LT1009 (Fig. 3C and D) resulted in a dose-dependent reduction in MVD, demonstrating that neutralization of endogenous S1P with the antibody mitigates VEFG/FGF-induced angiogenesis.

3.4. Immunohistochemical detection of S1P following laser-induced CNV

Having established that the anti-S1P mAbs were good tools to demonstrate the role of S1P in promoting in vitro and in vivo angiogenesis and after having demonstrated that CPECs respond to S1P, we used LT1009 to investigate whether tissue-specific S1P levels are increased in association with ocular pathology in the CNV lesion model (see Section 2). Fig. 4 shows representative images of S1P staining in uninjured control (panels A, B, C) and laser-injured (panels D, E, F) posterior cups. S1P immunoreactivity was detected in the CNV lesion (panels D and F) in the area of the vasculature (panel E) and neighboring tissue compared to the contralateral, non-injured control eye of the same animal (panels A, C). All cell types within the vascular lesion and in the wound bed surrounding the lesion contained cellular pools of S1P that were organized in a granular, punctate manner (Fig. 4; panels D–F). This S1P staining morphology is quite similar to that seen in isolated primary RPE and other ocular cells, which contain prominent intracellular pools of S1P that are organized in a similar granular, punctate manner (Swaney et al., 2008). Importantly, injured posterior cups exhibited a profound increase in S1P (Panel F) compared to non-injured tissue (panel C).

3.5. Effect of intravitreous anti-S1P on CNV lesion volume

In an initial pilot experiment, we evaluate the time-dependence of the CNV lesion formation and when the anti-S1P mAb was effective in mitigating the neovascularization. Fig. 5 shows typical fluorescent micrographs of CNV lesions taken from mouse eyes on day 7 (panels A and B), day 14 (panels C and D), and day 21 (panels E and F) following laser rupture of Bruch's membrane. The images shown in panels A, C and E represent flat-mounts of posterior cups from animals injected with non-specific isotype-matched (IgGk1) control antibody, whereas panels B, D and F illustrate the posterior cups from animals injected with the murine anti-S1P mAb, LT1002. Substantial reductions in the two-dimensional CNV lesions were observed only after specific LT1002 treatment. Furthermore, CNV lesion volumes as evaluated quantitatively by confocal microscopy were significantly reduced by 75% at day 7 post-laser burn, by 85% on day 14 post-laser and even further reduced by day 28 (panel G).

Having established that the antibodies had maximum effects 28 days after laser disruption of Bruch's membrane, a more extensive study (14–16 mice per group) was undertaken to compare LT1002 with the humanized form of anti-S1P mAb, LT1009. As shown in Fig. 6, the LT1002-treated animals exhibited a 66% reduction in CNV lesion volume compared to control antibody treatment. Interestingly, LT1009 was even more effective than LT1002 at reducing lesion volume, showing a 90% reduction in volume.

3.6. Effect of intravitreous anti-S1P on sub-retinal fibrosis

It is known that CNV lesions commonly evolve into scar over time as a consequence of the wound-healing process (Igarashi et al., 2003; Kent and Sheridan, 2003) and more importantly sub-retinal fibrosis contributes to visual acuity loss in exudative AMD. This

NIH-PA Author Manuscript

NIH-PA Author Manuscript

NIH-PA Author Manuscript

process is not addressed by currently available AMD treatments. Thus we evaluated whether LT1002 could mitigate sub-retinal scarring. The murine version of the anti-S1P mAb was chosen in order to obviate mouse against human immunogenicity responses that might complicate the fibrotic responses. Accordingly, LT1002 was tested for its ability to reduce collagen deposition in the CNV lesions. In micrographs of Masson's Trichrome-stained sections, extensive collagen deposition could be seen (blue staining) within and posterior to the vascular lesion by day 7 after laser injury in eyes treated with non-specific antibody (Fig. 7A). Most notably, the extent of collagen deposition was dramatically reduced in LT1002-treated eyes 7, 14 and 28 days after laser burn (Fig. 7B, C) and more closely resembled normal RPE and choroid (Fig. 7E). A quantitative analysis of collagen thickness is depicted in Fig. 7F, and demonstrates that LT1002 significantly ($p < 0.05$) reduced fibrosis in this model by 69%.

4. Discussion

The present study reveals, for the first time, that S1P is an important bioactive mediator that may have pleiotropic roles in a well-established animal model of exudative AMD. We demonstrate that S1P is expressed in the milieu surrounding choroidal neovascular tissue and that its expression is increased following laser disruption of Bruch's membrane. Enhanced expression of this very potent pro-angiogenic, pro-inflammatory and pro-fibrotic growth factor suggests that it may be an attractive target for intervention in this pathogenic process.

Accordingly, we found that intravitreous injection of either murine or humanized anti-S1P mAbs resulted in an 85% reduction in CNV lesion volume observed 14 days following laser injury, and almost complete suppression of CNV formation by 28 days post-laser injury.

We also demonstrate that S1P has direct effects on CPEC-associated tube formation and LT1009 can block tube formation in vitro, suggesting that the ability of anti-S1P mAbs to block CNV lesions is likely due to the ability of the antibodies to deprive S1P receptors of this pro-angiogenic ligand. Interestingly, the human CPEC we examined predominantly express $S1P_3$ receptors, while $S1P_1$ receptors are the more abundant receptor sub-type expressed by other vascular endothelial cells as reported in the literature (Chae et al., 2004; Maines et al., 2006; Sanchez and Hla, 2004; Sanchez et al., 2007). While our findings in LMEC and circulating endothelial precursor cells agree with these reports, endothelial cells isolated from human retinal vasculature express far more $S1P_3$ and $S1P_5$ than $S1P_1$. This suggests that vascular endothelium in the eye may differ from endothelium in other tissues. Thus, S1P receptor-specific antagonism as a therapeutic approach to drug treatment would have to be vascular bed-specific, as well. These findings argue in favor of ligand blockade rather than selective receptor antagonism and support the use of targeted antibodies such as LT1009.

The complement of S1P receptors on endothelial cells may be influenced by local S1P release during stress. The anti-angiogenic effects of the mAb in the CNV model can be explained by the ability of the mAb to neutralize S1P released locally by retinal cells, likely the RPEs. It is also possible that S1P could act indirectly as well by blocking the release and action of other locally produced pro-angiogenic growth factors such as VEGF, as has been seen in tumor angiogenesis models (Visentin et al., 2006).

The ability of the LT1009 to block in vivo neovascularization in Matrigel plugs supplanted with VEGF and FGF-2 (Fig. 1B), suggests not only that the anti-S1P mAb is effective in neutralizing systemic S1P and its direct effects on endothelial cells, but also indicates that the mAb can block the pro-angiogenic effects of VEGF and FGF-2.

NIH-PA Author Manuscript

NIH-PA Author Manuscript

NIH-PA Author Manuscript

In both the clinical setting and in animal models, a reduction in neovascularization results in diminished edema and leakage. VEGF is a well-recognized, important mediator of angiogenesis. VEGF is detected in both the experimental model of laser-induced CNV and surgically excised CNV tissues from patients with AMD (Frank, 1997; Kliffen et al., 1997; Ohno-Matsui et al., 2001; Otani et al., 2002). While a role for VEGF in CNV is well established, S1P has not been previously thought of as a mediator of pathologic ocular angiogenesis. By comparison to VEGF, S1P is pleiotropic in nature and a potent pro-angiogenic agent (Visentin et al., 2006). S1P enhances neovascularization via proliferation, migration and tubule formation of endothelial cells.

S1P is unusual in that it can function both as an extracellular signaling molecule and as an intracellular second messenger. The result presented in this study suggest that extracellular signaling is likely involved in ocular angiogenesis and that $S1P_3$ receptors might be the dominant receptor sub-type mediating the angiogenic effects of S1P on the vascular endothelial cells of the eye. $S1P_3$ receptors are GPCRs linked to G_i, G_q and $G_{12–13}$. Additional experiments will be required to elucidate the exact signaling mechanisms involved.

There appears to be substantial cross-talk among key pro-angiogenic growth factors. A number of growth factors activate sphingosine kinase-1 (SphK1), which converts sphingosine to S1P, including platelet derived growth factor, VEGF, nerve growth factor, tumor necrosis factor and FGF-2. Through VEGF receptor-2 (VEGFR-2) VEGF can stimulate extracellular signal-regulated kinase (ERK1/2) activation which in turn stimulates SphK1. The S1P that is generated activates Ras, in turn increasing Raf, MAPK/ERK kinase (MEK) and eventually DNA synthesis. S1P can activate VEGFR-2 in the absence of VEGF by receptor cross-talk. Ligand activation of the $S1P_2$ receptor leads to activation of Src, which results in phosphorylation of VEGFR2 (Tanimoto et al., 2002). This transactivation of VEGFR-2 causes activation of two signaling cascades that are important for movement and vascular remodeling. First, the activation of Src-family tyrosine kinases, the adaptor protein CrkII and Cas (Crk-associated substrate) and second PI3K-α, AKT pathway and eNOS resulting in formation of NO (Veikkola et al., 2000). After activation the $S1P_2$ receptor translocates to caveolae and concentrates with VEGFR-2 to facilitate eNOS phosphorylation and activation (Jobin et al., 2003). Furthermore, NO expression has been directly linked to angiogenesis potential.

Not only is there cross-talk between the S1P and VEGF signaling pathways, with S1P promoting the transactivation of VEGFR-2 (Tanimoto et al., 2002), but VEGF increases expression of $S1P_1$ receptors on endothelial cells, thereby sensitizing the endothelium to the actions of S1P and promoting endothelial viability (Ferrara et al., 2006; Kee et al., 2005; Radeff-Huang et al., 2004). S1P also up-regulates TIMP and integrin expression further promoting vascularization and vascular remodeling (Bayless and Davis, 2003; Granata et al., 2007; Skoura et al., 2007; Walter et al., 2007).

While S1P affects vascular permeability in a tissue-specific manner depending on which isoforms of the S1P receptors are expressed, Hla and co-workers have recently provided evidence suggesting that S1P may promote vascular permeability via $S1P_2$ receptors in the pulmonary and ocular vascular beds (Sanchez et al., 2007; Skoura et al., 2007). These effects were Rho-ROCK-PTEN-dependent and involved inhibition of VE-cadherens phosphorylation and resulting translocation to adherens junctions.

Of particular interest is the recent finding that inhibition of SphK was found to both suppress VEGF-induced vascular leakage in the Miles mouse model of vascular permeability and reduce retinal vascular leakage in a rat diabetic retinopathy model (Maines et al., 2006). In

NIH-PA Author Manuscript

NIH-PA Author Manuscript

NIH-PA Author Manuscript

various tumor models of angiogenesis, we have demonstrated that S1P is more potent than VEGF or FGF-2 and appears to be permissive on VEGF action (Visentin et al., 2006), likely due to the observed transactivation of VEGF receptors by S1P (Igarashi et al., 2003; Tanimoto et al., 2002).

S1P has well-known pro-inflammatory effects including the induction of the pro-inflammatory cytokines and factors, TNF-α, IL-6, IL-8, monocyte chemotactic protein-1, platelet activating factor, COX and PGE_2 (Ferrara et al., 2006; Kee et al., 2005). Many of these mediators are also pro-angiogenic. Although not addressed directly in the present study, one may predict that interfering with S1P signaling may have the added benefit of reducing the inflammatory responses that contribute to many ocular disorders, including AMD.

Another potential advantage of targeting S1P is that, in contrast to VEGF, S1P is believed to be pro-fibrotic. For example, S1P is known to activate multiple fibroblast lineages of non-ocular origins (Hobson et al., 2001; Keller et al., 2007; Olivera et al., 1999; Urata et al., 2005; Wang et al., 1997). In addition, S1P exhibits cross-talk with other pro-fibrotic mediators like platelet derived growth factor and TGF-β, promotes expression connective tissue growth factor and up-regulates TIMP1 (Ferrara et al., 2006; Kee et al., 2005; Radeff-Huang et al., 2004). Consequently, it is not difficult to imagine that choroidal-derived fibroblasts and RPE cells may respond to S1P by laying down collagen during scar formation. A companion paper published from our laboratory demonstrates the expression of $S1P_{1–3,5}$ and SphK1 by multiple human primary ocular cells, particularly in RPE cells (Swaney et al., 2008). It was also demonstrated that S1P promotes the RPE cell proliferation in a dose- and time-dependent manner and induces transformation of RPE cells to the pro-fibrotic (myofibroblast) cell phenotype. Also, S1P stimulates the expression of plasminogen activator inhibitor-1 (PAI-1) and heat shock protein 47 (HSP47), two proteins that are linked to increased tissue fibrosis. This finding is consistent with the study of Fig. 7, showing that the murine anti-S1P mAb substantially reduces the fibrogenic effects of S1P in vivo. These data, while preliminary, are consistent with the in vitro findings from our laboratory (Swaney et al., 2008) showing direct effects of S1P on ocular fibroblasts. We hypothesize that increased levels of S1P that were observed in injured eyes could contribute to AMD by promoting scar formation via these direct effects on ocular fibroblasts. In fact, the RPE cells might not only participate in the fibrogenic response to S1P, but the current work suggests that RPEs might also be a major source of S1P in injured eyes.

Although the exact pathogenesis of CNV remains incompletely understood, aspects of this CNV model recapitulate the angiogenesis, inflammation and sub-retinal fibrosis seen in exudative AMD. In the clinical setting of CNV, the scarring response irreversibly damages photoreceptors and treatments that modify this response may help preserve or even rescue photoreceptors. We demonstrate for the first time that S1P is a mediator of angiogenesis and we strongly suspect that it will also promote sub-retinal fibrosis in this model of AMD. This is consistent with findings from other organs and diseases states where S1P has been shown to play a role in these processes.

Ideally treatment modalities for exudative AMD would target the multiple mechanisms of AMD associated vision loss. Although the pan-VEGF inhibitors are quite effective, they are singly targeted against only one signaling system and there is potential need to address other signaling systems involved in pathogenic angiogenesis. Because S1P appears to influence the additive and synergistic effects of neovascularization, inflammation, fibrosis and enhanced vascular permeability resulting in tissue damage, targeting the S1P signaling system should be valuable.

NIH-PA Author Manuscript

NIH-PA Author Manuscript

NIH-PA Author Manuscript

In conclusion, considering S1P as a novel target may lead to a more effective therapeutic strategy for treatment of diseases associated with pathologic neovascularization. Our approach of neutralizing S1P by the use of specific anti-S1P antibodies addresses a neovascularization pathway separate from that activated by VEGF, and thus may serve in combination therapy with anti-VEGF agents such as ranibizumab. Based on the known biochemistry of S1P, our humanized anti-S1P therapeutic mAb could have additional positive effects on CNV associated with AMD as the result of their anti-scarring and anti-inflammatory effects, thus acting as its own combination therapy. Considering that the anti-S1P mAb at an effective dose of 0.5 μg/eye almost completely abrogated the CNV lesions, targeting S1P with this novel antibody may offer a more effective therapeutic approach than currently exists with anti-VEGF agents. A Phase 1 safety trial activities in AMD have been initiated using the humanized anti-S1P mAb, LT1009.

Acknowledgments

The authors thank Lynn Shaw, University of Florida, for important help initiating the CNV studies and help with preparation of the manuscript; Steve Searle, Sanger Centre, Cambridge for use of the sequence analysis program SR7.6; and Dr. H. Brad Cunningham for providing the rabbit eyes and plasma for the examination of vitreous and plasma studies of S1P.

Abbreviations

AMD	Age-related macular degeneration
FGF-2	basic fibroblast growth factor
CNV	choroidal neovascularization
CPEC	brain choroidal plexus endothelial cells
EPC	endothelial progenitor cells
LMEC	lung microvascular endothelial cells
mAb	monoclonal antibody
RPE	retinal pigmented epithelium
HREC	retinal vascular endothelial cells
S1P	sphingosine-1-phosphate
SphK1	sphingosine kinase type 1
VEGF	vascular endothelial growth factor

References

Anliker B, Chun J. Lysophospholipid G protein-coupled receptors. J Biol Chem. 2004; 279 (20): 20555–20558. [PubMed: 15023998]

Augustin AJ, Offermann I. Emerging drugs for age-related macular degeneration. Expert Opin Emerg Drugs. 2006; 11 (4):725–740. [PubMed: 17064228]

Bayless KJ, Davis GE. Sphingosine-1-phosphate markedly induces matrix metalloproteinase and integrin-dependent human endothelial cell invasion and lumen formation in three-dimensional collagen and fibrin matrices. Biochem Biophys Res Commun. 2003; 312 (4):903–913. [PubMed: 14651957]

Bernatchez PN, et al. Sphingosine 1-phosphate effect on endothelial cell PAF synthesis: role in cellular migration. J Cell Biochem. 2003; 90 (4):719–731. [PubMed: 14587028]

Caballero S, et al. Ischemic vascular damage can be repaired by healthy, but not diabetic, endothelial progenitor cells. Diabetes. 2007; 56 (4):960–967. [PubMed: 17395742]

NIH-PA Author Manuscript

NIH-PA Author Manuscript

NIH-PA Author Manuscript

Chae SS, et al. Constitutive expression of the S1P1 receptor in adult tissues. Prostaglandins Other Lipid Mediat. 2004; 73 (1–2):141–150. [PubMed: 15165038]

Chang KH, et al. IGF binding protein-3 regulates hematopoietic stem cell and endothelial precursor cell function during vascular development. Proc Natl Acad Sci USA 104 (25). 2007:10,595–10,600.

Cyster JG. Chemokines, sphingosine-1-phosphate, and cell migration in secondary lymphoid organs. Annu Rev Immunol. 2005; 23:127–159. [PubMed: 15771568]

Ferrara N, et al. Development of ranibizumab, an anti-vascular endothelial growth factor antigen binding fragment, as therapy for neovascular age-related macular degeneration. Retina. 2006; 26 (8):859–870. [PubMed: 17031284]

Frank RN. Growth factors in age-related macular degeneration: pathogenic and therapeutic implications. Ophthalmic Res. 1997; 29 (5):341–353. [PubMed: 9323725]

Garcia JG, et al. Sphingosine 1-phosphate promotes endothelial cell barrier integrity by Edg-dependent cytoskeletal rearrangement. J Clin Invest. 2001; 108 (5):689–701. [PubMed: 11544274]

Gardell SE, et al. Emerging medicinal roles for lysophospholipid signaling. Trends Mol Med. 2006; 12 (2):65–75. [PubMed: 16406843]

Granata R, et al. Insulin-like growth factor binding protein-3 induces angiogenesis through IGF-I- and SphK1-dependent mechanisms. J Thromb Haemost. 2007; 5 (4):835–845. [PubMed: 17388800]

Grant MB, Guay C. Plasminogen activator production by human retinal endothelial cells of nondiabetic and diabetic origin. Invest Ophthalmol Vis Sci. 1991; 32:53–64. [PubMed: 1702773]

Hobson JP, et al. Role of the sphingosine-1-phosphate receptor EDG-1 in PDGF-induced cell motility. Science. 2001; 291 (5509):1800–1803. [PubMed: 11230698]

Igarashi J, et al. VEGF induces S1P1 receptors in endothelial cells: implications for cross-talk between sphingolipid and growth factor receptors. Proc Natl Acad Sci USA. 2003; 100(19):10,664–10,669. [PubMed: 12506193]

Jobin CM, et al. Receptor-regulated dynamic interaction between endothelial nitric oxide synthase and calmodulin revealed by fluorescence resonance energy transfer in living cells. Biochemistry. 2003; 42(40):11,716–11,725. [PubMed: 12515535]

Kee TH, et al. Sphingosine kinase signalling in immune cells. Clin Exp Pharmacol Physiol. 2005; 32 (3):153–161. [PubMed: 15743396]

Keller CD, et al. Immunomodulator FTY720 induces myofibroblast differentiation via the lysophospholipid receptor S1P3 and Smad3 signaling. Am J Pathol. 2007; 170 (1):281–292. [PubMed: 17200201]

Kent D, Sheridan C. Choroidal neovascularization: a wound healing perspective. Mol Vis. 2003; 9:747–755. [PubMed: 14735062]

Kliffen M, et al. Increased expression of angiogenic growth factors in age-related maculopathy. Br J Ophthalmol. 1997; 81 (2):154–162. [PubMed: 9059252]

Langlois S, et al. Membrane type 1-matrix metalloproteinase (MT1-MMP) cooperates with sphingosine 1-phosphate to induce endothelial cell migration and morphogenic differentiation. Blood. 2004; 103 (8):3020–3028. [PubMed: 15070679]

Lee H, et al. Lysophosphatidic acid and sphingosine 1-phosphate stimulate endothelial cell wound healing. Am J Physiol Cell Physiol. 2000; 278 (3):C612–C618. [PubMed: 10712250]

Li Y, et al. Interaction of cortactin and Arp2/3 complex is required for sphingosine-1-phosphate-induced endothelial cell remodeling. Exp Cell Res. 2004; 298 (1):107–121. [PubMed: 15242766]

Limaye V, et al. Sphingosine kinase-1 enhances endothelial cell survival through a PECAM-1-dependent activation of PI-3K/Akt and regulation of Bcl-2 family members. Blood. 2005; 105 (8): 3169–3177. [PubMed: 15632208]

Maines LW, et al. Pharmacologic manipulation of sphingosine kinase in retinal endothelial cells: implications for angiogenic ocular diseases. Invest Ophthalmol Vis Sci. 2006; 47 (11):5022–5031. [PubMed: 17065523]

Ohno-Matsui K, et al. Novel mechanism for age-related macular degeneration: an equilibrium shift between the angiogenesis factors VEGF and PEDF. J Cell Physiol. 2001; 189 (3):323–333. [PubMed: 11748590]

NIH-PA Author Manuscript

NIH-PA Author Manuscript

NIH-PA Author Manuscript

Olivera A, et al. Sphingosine kinase expression increases intracellular sphingosine-1-phosphate and promotes cell growth and survival. J Cell Biol. 1999; 147 (3):545–558. [PubMed: 10545499]

Olivera A, Rivera J. Sphingolipids and the balancing of immune cell function: lessons from the mast cell. J Immunol. 2005; 174 (3):1153–1158. [PubMed: 15661867]

Otani A, et al. Vascular endothelial growth factor family and receptor expression in human choroidal neovascular membranes. Microvasc Res. 2002; 64 (1):162–169. [PubMed: 12074642]

Ozaki H, et al. Sphingosine-1-phosphate signaling in endothelial activation. J Atheroscler Thromb. 2003; 10 (3):125–131. [PubMed: 14564080]

Radeff-Huang J, et al. G protein mediated signaling pathways in lysophospholipid induced cell proliferation and survival. J Cell Biochem. 2004; 92 (5):949–966. [PubMed: 15258918]

Rosenfeld PJ, et al. Ranibizumab: phase III clinical trial results. Ophthalmol Clin North Am. 2006; 19 (3):361–372. [PubMed: 16935211]

Sabbadini RA. Targeting sphingosine-1-phosphate for cancer therapy. Br J Cancer. 2006; 95 (9):1131–1135. [PubMed: 17024123]

Sanchez T, Hla T. Structural and functional characteristics of S1P receptors. J Cell Biochem. 2004; 92 (5):913–922. [PubMed: 15258915]

Sanchez T, et al. Induction of vascular permeability by the sphingosine-1-phosphate receptor-2 (S1P2R) and its downstream effectors ROCK and PTEN. Arterioscler Thromb Vasc Biol. 2007; 27 (6):1312–1318. [PubMed: 17431187]

Sengupta N, et al. The role of adult bone marrow-derived stem cells in choroidal neovascularization. Invest Ophthalmol Vis Sci. 2003; 44 (11):4908–4913. [PubMed: 14578416]

Skoura A, et al. Essential role of sphingosine 1-phosphate receptor 2 in pathological angiogenesis of the mouse retina. J Clin Invest. 2007; 117 (9):2506–2516. [PubMed: 17710232]

Spiegel S, Milstien S. Sphingosine-1-phosphate: an enigmatic signalling lipid. Nat Rev Mol Cell Biol. 2003; 4 (5):397–407. [PubMed: 12728273]

Swaney JS, Moreno KM, Gentile AM, Sabbadini RA, Stoller GL. Sphingosine-1-phosphate (S1P) is a novel fibrotic mediator in the eye. Exp Eye Res. 2008; 87 (4):367–375. [PubMed: 18687328]

Tanimoto T, et al. Transactivation of vascular endothelial growth factor (VEGF) receptor Flk-1/KDR is involved in sphingosine 1-phosphate-stimulated phosphorylation of Akt and endothelial nitric-oxide synthase (eNOS). J Biol Chem. 2002; 277(45):42,997–43,001.

Urata Y, et al. Sphingosine 1-phosphate induces alpha-smooth muscle actin expression in lung fibroblasts via Rho-kinase. Kobe J, Med, Sci. 2005; 51 (1–2):17–27. [PubMed: 16199931]

Veikkola T, et al. Regulation of angiogenesis via vascular endothelial growth factor receptors. Cancer Res. 2000; 60 (2):203–212. [PubMed: 10667560]

Visentin B, et al. Validation of an anti-sphingosine-1-phosphate antibody as a potential therapeutic in reducing growth, invasion, and angiogenesis in multiple tumor lineages. Cancer Cell. 2006; 9 (3): 225–238. [PubMed: 16530706]

Walter DH, et al. Sphingosine-1-phosphate stimulates the functional capacity of progenitor cells by activation of the CXCR4-dependent signaling pathway via the S1P3 receptor. Arterioscler Thromb Vasc Biol. 2007; 27 (2):275–282. [PubMed: 17158356]

Wang F, et al. Sphingosine 1-phosphate stimulates rho-mediated tyrosine phosphorylation of focal adhesion kinase and paxillin in Swiss 3T3 fibroblasts. Biochem J. 1997; 324 (Pt 2):481–488. [PubMed: 9182707]

Watterson KR, et al. Regulation of fibroblast functions by lysophospholipid mediators: potential roles in wound healing. Wound Repair Regen. 2007; 15 (5):607–616. [PubMed: 17971005]

Zarbin MA. Functionalizing cell-based therapy for age-related macular degeneration. Am J Ophthalmol. 2007; 143 (4):681–682. [PubMed: 17386276]

NIH-PA Author Manuscript
NIH-PA Author Manuscript
NIH-PA Author Manuscript

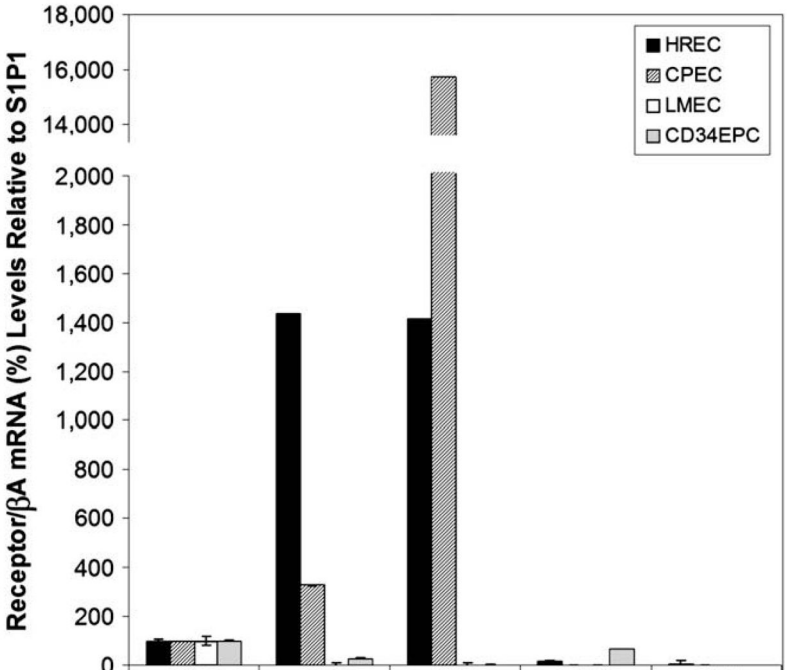

	S1P1	S1P2	S1P3	S1P4	S1P5
HREC	100	1,432	1,414	15.4	4.2
CPEC	100	327	15,682	0.06	1.43
LMEC	100	0.16	1.30	0.004	0.002
CD34EPC	100	27.9	0.28	65.5	

Fig. 1.

CPEC express receptors for S1P. Quantitative real-time PCR of the cognate S1P receptors expressed by diverse human vascular endothelial cells. RT-PCR data are plotted showing relative $S1PR_{1–5}$ expression in HREC, CPEC and LMEC. Human HREC and CPEC express significantly higher levels of $S1P_2$ and $S1P_3$ mRNA by comparison to $S1P_1$, with $S1P_3$ being by far the most abundant of all the S1P receptors expressed by CPEC. Both LMEC and $CD34^+$ EPC express $S1P_1$ most abundantly. All samples were normalized to b-actin and studies were performed in triplicate. The data represent mean values ± SEM that are relative to $S1P_1$ receptor expression.

NIH-PA Author Manuscript
NIH-PA Author Manuscript
NIH-PA Author Manuscript

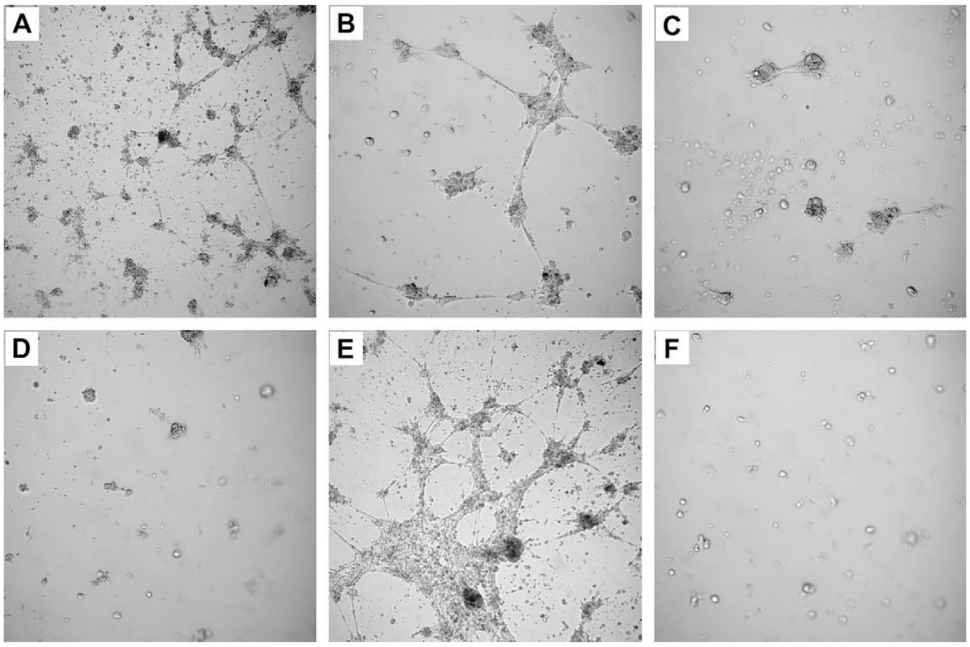

Fig. 2.

LT1009 inhibits tube formation in vitro. CPEC, either unstimulated or pre-incubated with S1P with or without LT1009, were plated on Matrigel-coated wells and allowed to incubate for 12 h. S1P alone (1 nM or 10 nM, A and B, respectively) stimulated tube formation, compared to unstimulated cells (F). Co-incubation of 10 nM S1P with 25 μg/mL LT1009 (C) greatly reduced microvessel tube formation by these cells, while 50 μg/mL LT1009 (D) completely abrogated tube formation. (E) A positive control (CPEC in the presence 50 ng/mL VEGF and 50 ng/mL FGF-2). All phase contrast micrographs are typical of at least three wells per condition, and were taken at 10× original magnification.

NIH-PA Author Manuscript
NIH-PA Author Manuscript
NIH-PA Author Manuscript

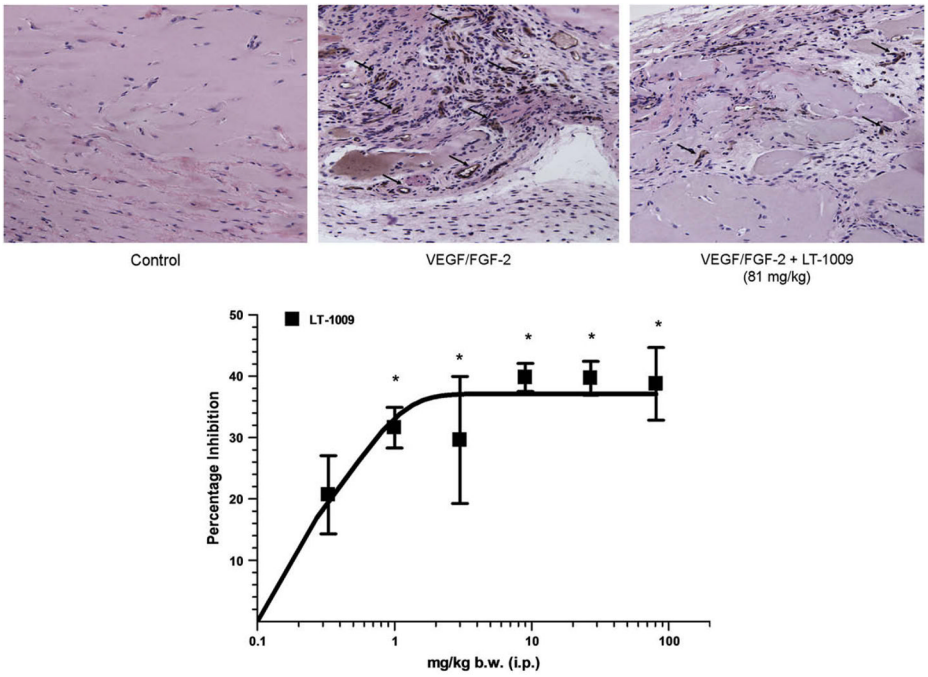

Fig. 3.

LT1009 shows efficacy in the in vivo Matrigel neovascularization assay by reducing microvascular vessel formation induced by the pro-angiogenic factors VEGF and FGF-2. Matrigel plugs loaded with 50 ng/mL VEGF and 50 ng/mL FGF-2 were implanted in female C57BL/6 mice. Mice received drug treatments consisting of equal volumes of 0.33–81 mg/kg LT1009 or saline beginning 1 day prior to the implantation of Matrigel plugs; each treatment was then administered intraperitoneally twice daily for 14 days. At the end of the experiment, the plugs were collected, sectioned and stained for CD31. (A) Representative image of sections from controls. (B) Representative image of sections from mice harboring VEGF/FGF-2 loaded plugs; black arrows indicate representative vessels. (C) Representative image of sections from mice harboring VEGF/FGF-2 loaded plugs and treated with LT1009; note the reduced number of vessels (black arrows). (D) Quantification of the reduction of microvascular density (MVD) in the plugs ($n \geq 6$ plugs per treatment). Statistical analysis was performed using 1-way ANOVA (***$p < 0.0001$) followed by Bonferroni's post test (*$p < 0.01$).

NIH-PA Author Manuscript
NIH-PA Author Manuscript
NIH-PA Author Manuscript

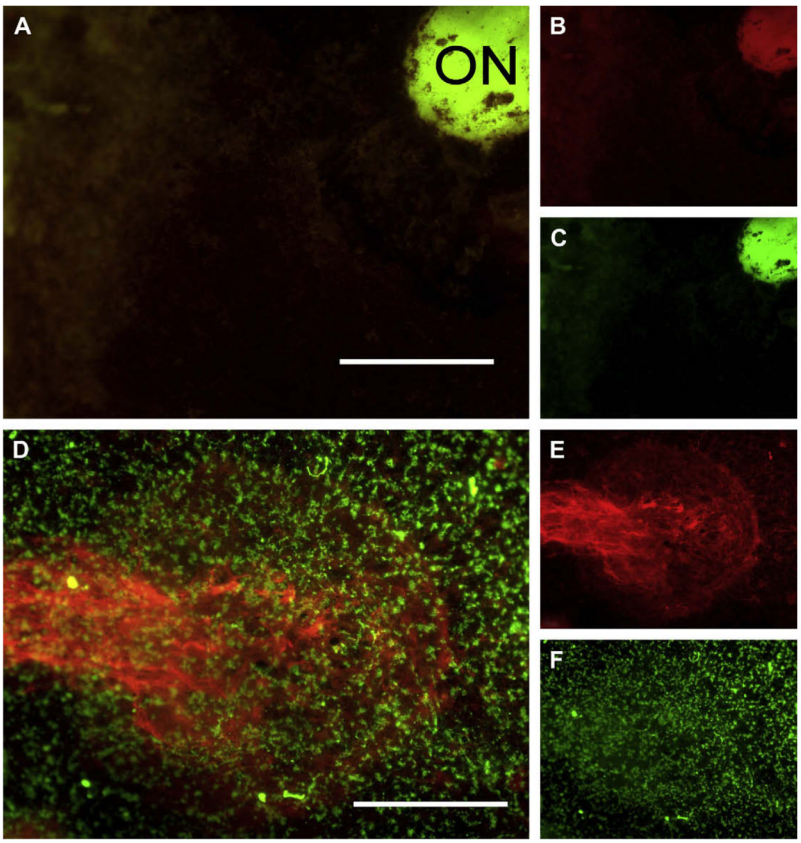

Fig. 4.

Immunohistochemical localization of S1P in the murine retina. (A) Composite image of red (B) and green (C) channels of a posterior cup from an uninjured (negative control) eye reacted with rhodamine-conjugated agglutinin, S1P antibody and FITC-conjugated secondary antibody. (D) Composite image of red (E) and green (F) channels of a posterior cup from an eye that underwent laser rupture of Bruch's membrane, and reacted as described above for the eye in panels A, B, C. Note the lack of S1P immunoreactivity in the untreated control eye and widespread S1P immunoreactivity in the laser-treated eye in association with the CNV lesion. Scale bar = 50 μm.

NIH-PA Author Manuscript
NIH-PA Author Manuscript
NIH-PA Author Manuscript

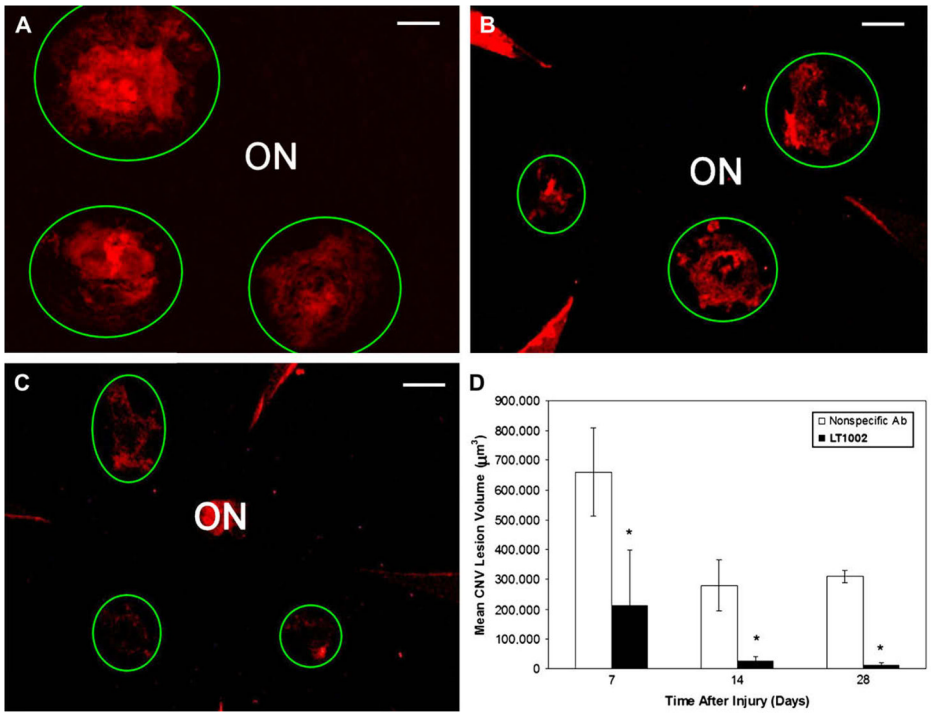

Fig. 5.

Time-dependent efficacy of the anti-S1P mAb LT1002 in reducing CNV lesions in vivo. CNV lesion volume was measured on days 7, 14 and 28 after laser rupture of Bruch's membrane (3 burns/eye, 1 eye per animal). The areas for each burn were converted to a volume and the volumes averaged to produce a single CNV lesion volume for each animal. Representative fluorescent micrographs of flat-mounted posterior eye cups from injured eyes stained for with *R. communis* agglutinin are shown. (A), (C) and (E) depict eyes that received non-specific antibody 7, 14 and 28 days post injury, respectively. (B), (D) and (F) depict eyes treated with intravitreal injection of 0.5 μg per eye of LT1002 7, 14, and 28 days post injury, respectively. (G) CNV lesion size at all time points was quantified and is shown in graph form. * Denotes $p < 0.05$ compared to non-specific antibody at days 7, 14 and 28. Scale bar in (A) = 50 μm and is applicable to all of the micrographs. $n = 3$ animals per treatment condition at each time point.

NIH-PA Author Manuscript

NIH-PA Author Manuscript

NIH-PA Author Manuscript

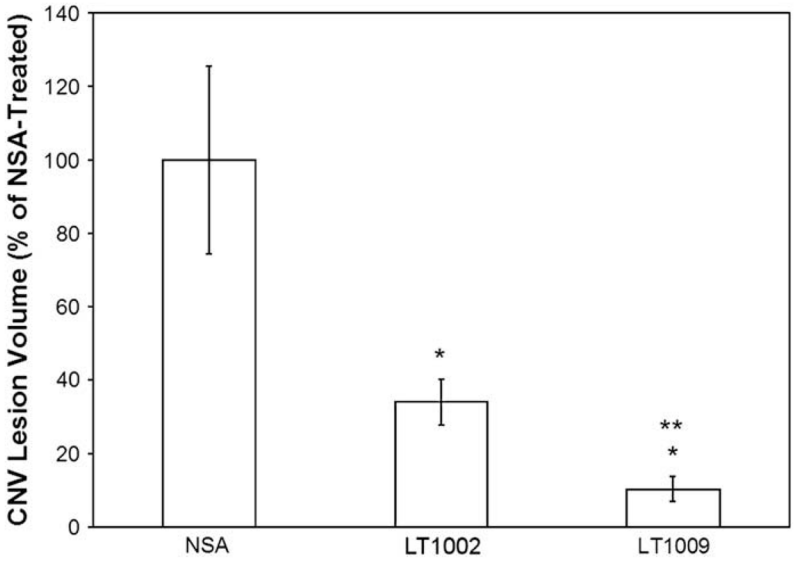

Fig. 6.

A comparison of LT1002 and LT1009 efficacy on reducing experimental CNV lesion volume in mouse eyes injured by laser rupture of Bruch's membrane. All animals received intravitreal injection of either non-specific antibody (NSA), injection of 0.5 μg per eye of LT1002 or LT1009 at the time of injury and weekly thereafter for the duration of the experiment. At this time point (28 days post injury) weekly injections of LT1009 were three-fold more effective than weekly injections of LT1002. $n = 15$ for non-specific antibody, $n = 16$ for LT1002, and $n = 14$ for LT1009. * Denotes $p < 0.05$ compared to non-specific antibody. ** Denotes $p < 0.05$ compared to LT1002.

NIH-PA Author Manuscript
NIH-PA Author Manuscript
NIH-PA Author Manuscript

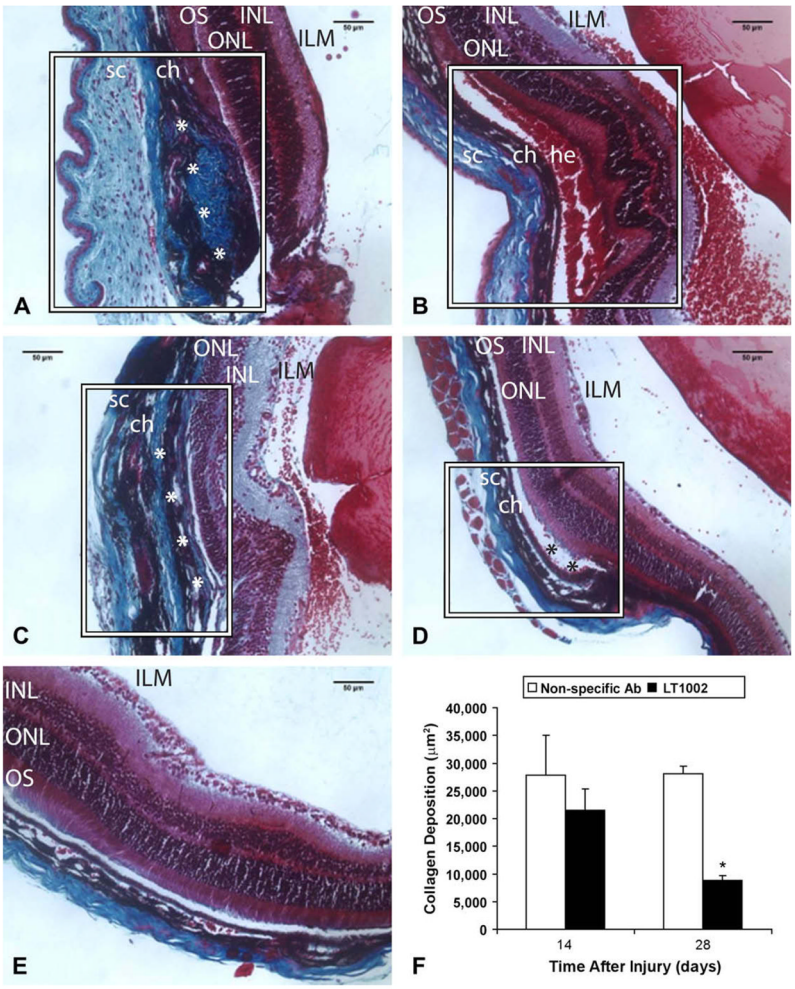

Fig. 7.

Use of LT1002 resulted in a reduction of scarring in the CNV wound bed. Cross sections stained with Masson's Trichrome. Lesions are shown within the white box. Histological images show collagen deposition (blue staining) within and posterior to the vascular lesion after laser injury in eyes treated with 0.5 μg per eye of non-specific antibody on day 7 (A), and compared to LT1002-treated (0.5 μg) eyes on days 7 (B), 14 (C) and 28 (D). (E) A naive (untreated control) eye for comparison. OS, outer segments; ONL, outer nuclear layer; INL, inner nuclear layer; ILM, internal limiting membrane; sc, sclera; ch, choroid; he, hemorrhage; *Representative locations where collagen deposition was measured. (F) A summary plot of the collagen deposition measurements in all eyes examined ($n = 3$ eyes per treatment condition at each time point). * Denotes $p < 0.05$ versus treatment with nonspecific antibody.

NIH-PA Author Manuscript

NIH-PA Author Manuscript

NIH-PA Author Manuscript

Table 1

S1P concentrations in vitreous and plasma of naive rabbits, as measured by ELISA

	S1P concentration (μM)
Plasma	1.08 ± 0.05 (*n* = 10)
Vitreous	0.12 ± 0.01 (*n* = 10)